PHILOSOPHICAL MAGAZINE A, 2002, VOL. 82, NO. 5, 943–954

Spatio-temporal instabilities of the Kirkendall marker planes during interdiffusion in β'-AuZn

M. J. H. VAN DAL, A. M. GUSAK†, C. CSERHÁTI‡, A. A. KODENTSOV and F. J. J. VAN LOO§

Laboratory of Solid State and Materials Chemistry, Eindhoven University of Technology, PO Box 513, 5600 MB Eindhoven, The Netherlands

[*Received 29 January 2001 and accepted in revised form 17 August 2001*]

ABSTRACT

A Kirkendall-effect-mediated behaviour (migration) of fiducial markers originally situated at the contact surface of a diffusion couple can be complex in both temporal and spatial domains. A phenomenological approach based on a concept of the Kirkendall velocity construction is used to rationalize the movement of the inert markers upon diffusion-controlled growth of the β'-AuZn intermetallic phase. It is demonstrated (experimentally as well as theoretically) that the Kirkendall marker planes can be multiple, stable or unstable within the single-phase reaction product. A general criterion of the microstructural instability of the Kirkendall plane is introduced.

§ 1. INTRODUCTION

The present study originates in the quest for experimental proof for the existence of multiple Kirkendall planes upon interdiffusion in single-phase materials.

The elucidation of the Kirkendall effect manifestations is of fundamental importance because it contributes greatly to the understanding of interdiffusion in solids. There are at least four major technological fields in which this subject is paramount: structural engineering components; ceramic–metal-matrix and other composites; coating technologies; microelectronic devices. The Kirkendall effect accompanying interactions between constituents of such hybrid structures at elevated temperatures can, for example, induce stress and even deformation on a macroscopic scale (Stephenson 1988, Daruka *et al.* 1996). It can also cause migration of macroscopic inclusions inside a reaction zone, development of a diffusion porosity and periodic pattern formation (Kodentsov *et al.* 1998). For further progress in these fields it is imperative to be able to predict (and control) the possible microstructural developments associated with the Kirkendall effect.

Since the discovery of this effect in 1947 (Smigelskas and Kirkendall 1947) and the following analysis by Darken (1948), various manifestations of the Kirkendall effect have been explored in a large number of carefully controlled experiments (see, for example, Philibert (1991)). It is important to remark right away that the micro-

---

† On leave from Cherkassy State University, Ukraine

‡ On leave from Department of Solid State Physics, Debrecen University, Hungary.

§ Author for correspondence. Email: F.J.J.v.Loo@tue.nl

Philosophical Magazine A ISSN 0141–8610 print/ISSN 1460-6992 online
http://www.tandf.co.uk/journals
DOI: 10.1080/01418610110094752

structural stability and uniqueness of the Kirkendall marker plane have not been questioned for quite a long time. It was left to Cornet and Calais (1972) and van Loo *et al.* (1990) to describe hypothetical diffusion couples in which several 'Kirkendall marker planes' can emerge.

Recently a clear-cut experimental verification of these ideas was found by van Dal *et al.* (2000a, b) in multiphase systems. For example, in the Ni–Ti and Co–Si systems it was shown that Kirkendall planes as marked by inert particles, placed prior to the annealing at the contact surface of a diffusion couple, can be multiple, stable or unstable. In order to rationalize the Kirkendall-effect-mediated behaviour of macroscopic inclusions inside a diffusion zone, a phenomenological approach based on the concept of the Kirkendall velocity curve has been introduced (van Dal *et al.* 2000b).

The overriding objective in writing this paper was to make clear that also in a single-phase diffusion layer the Kirkendall plane need not be unique. More than one Kirkendall marker plane can show up within a single-phase reaction product and, under certain conditions, the inert markers do not accumulate at a well-defined location of the diffusion zone, that is the Kirkendall plane does not exist at all in such a couple.

In this respect, the β'-ordered phase (B2 structure) of the binary Au–Zn system attracts special attention. Previous reports about interdiffusion in this intermetallic compound (T. Shimozaki 1993, private communication, Shimozaki *et al.* 1993) indicate a rather unusual behaviour of inert markers in the β'-AuZn phase layer developed during interaction between pure Au and the γ-'$AuZn_2$' phase containing 64 at.% Zn. The Kirkendall markers (W wires about 5 μm thick) and the 'original interface revealed by traces of the joining plane' (presumably by grinding debris remaining at the contact surface between the couple halves) were observed at two different locations inside the β'-AuZn reaction layer. This conspicuous finding was, however, not identified by these workers as the formation of the multiple Kirkendall planes, and this phenomenon was not critically examined.

Therefore, the aims of the present communication are as follows:

(i) to demonstrate variation in the Kirkendall marker plane appearance inside a single-phase product layer of β'-AuZn by changing the initial composition of the end members of the reaction couple;

(ii) to present a framework for understanding and rationalizing the Kirkendall marker behaviour using the concept of the Kirkendall velocity construction.

§ 2. EXPERIMENTAL PROCEDURE

Pure (99.9995%) Au supplied by Alfa products, Germany and pure (99.98%) Zn supplied by Merck, Germany were used as starting materials.

A number of binary Au–Zn alloys were melted at 800–1000°C in alumina crucibles in a flowing Ar gas atmosphere under flux consisting of $ZnCl_2$ and NaCl (mass ratio, 3 : 1). The alloy ingots were mechanically shaped into a form (usually disc like) suitable for the use as diffusion couple end members. After shaping, the couple halves were equilibrated at 500°C under a flowing Ar + 5 vol.% H_2 gas mixture for 24–48 h.

The bonding faces of the couple halves were ground flat and polished to a finish with 0.25 μm alumina slurry. The polished metal surfaces were ultrasonically cleaned in ethanol and dried in hot air.

The diffusion couples were prepared at 500°C under a flowing Ar + 5 vol.% H_2 gas mixture in specially designed steel clamps. This clamp, which keeps the end members of the couple in intimate contact during annealing, was placed in the hot zone of a horizontal tube furnace. After a diffusion anneal, this clamp can be rapidly removed from the furnace and immediately quenched in cold water. Prior to annealing, small particles (0.5–5 μm) of ThO_2 were introduced as inert markers between the initial end members. In all experiments the temperature was controlled within ±3°C.

After heat treatment and standard metallographic preparation, cross-sections of the couples were examined by optical microscopy, scanning electron microscopy (SEM) and electron probe microanalysis (EPMA).

§ 3. RESULTS AND DISCUSSION

3.1. *The marker velocity construction and formation of multiple Kirkendall planes*

The Kirkendall-effect-induced mass flow can be best visualized by the motion of fiducial markers placed along the anticipated zone of interdiffusion. During interaction, such markers will move with a so-called Kirkendall velocity relative to a laboratory (or Matano) frame of reference, that is with respect to one end of the diffusion couple. In the case of an A–B couple, the Kirkendall velocity v is dependent on the difference in intrinsic diffusivities of the species involved and the concentration gradients developing in the interdiffusion zone (Darken 1948):

$$v = V_B(D_B - D_A)\frac{\partial C_B}{\partial x}. \tag{1}$$

D_i($m^2 s^{-1}$) is the intrinsic diffusion coefficient of component i, defined by $J_i = -(\partial C_i/\partial x)$ with J_i being the intrinsic flux with respect to the Kirkendall frame of reference and C_i ($mol\,m^{-3}$) is the concentration of component i. V_i ($m^3\,mol^{-1}$) is the partial molar volume of component i and x(m) is the position parameter.

In a diffusion-controlled interaction, the inert markers positioned at the location of the Kirkendall plane are the only markers that stay at a constant composition and move parabolically in time with a velocity

$$v_K = \frac{dx}{dt} = \frac{x_K}{2t} \tag{2}$$

(x_K is the distance between the position of the marker and Matano plane $x = 0$).

Obviously, the position (and velocity) of the Kirkendall plane after the interdiffusion time t can be found graphically just as the point of intersection between the marker velocity plot and the straight line $v = x/2t$ (Cornet and Calais 1972).

At this point it is appropriate to mention some features of the β'-AuZn intermetallic compound relevant to this discussion. The β'-ordered phase (B2; CsCl structure) in the binary Au–Zn system exists in a wide homogeneity range (e.g. at 500°C this is approximately 38.0–57.0 at.% Zn (Okamoto and Massalski 1988)), and the diffusivities of the components are strongly composition dependent. Of particular importance is that, according to self-diffusion measurements using ^{65}Zn and ^{195}Au radiotracers reported by Gupta and Lieberman (1971), Au is the faster-diffusing species in the Au-rich part of the β' phase, whereas Zn atoms a have higher mobility in the Zn-rich part. In this situation, the Kirkendall velocity within the β' intermetallic layer diffusion grown from its adjacent phases will change direction (see equation (1), with A = Au and B = Zn).

Figure 1 (*a*) shows a representative microstructure of the reaction zone developed during interaction at 500°C in a diffusion couple based on pure Au and γ-AuZn$_2$

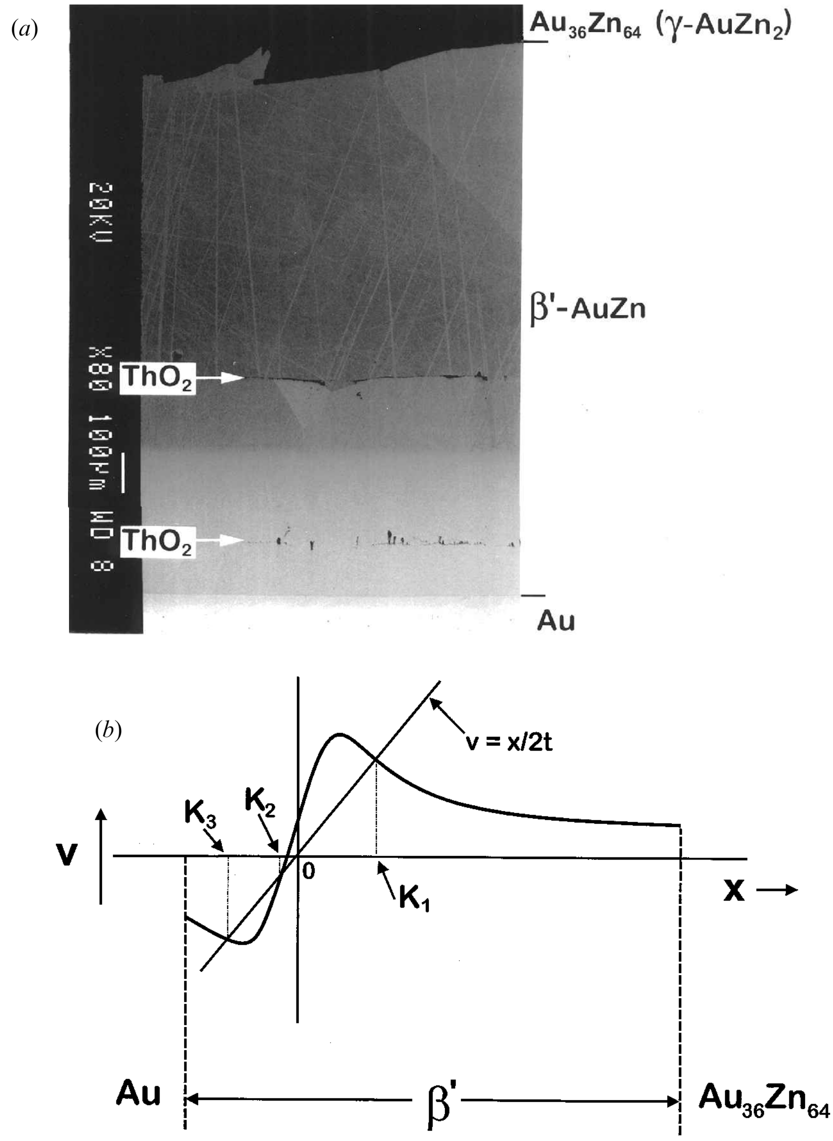

Figure 1. (*a*) Back-scattered electron image (BEI) of the diffusion zone after interaction. (*b*) The Kirkendall velocity curve corresponding to the β'-AuZn product layer in the annealed (500°C; 17.25 h; Ar + 5 vol.% H_2) Au–$Au_{36}Zn_{64}$ (γ-'$AuZn_2$') couple constructed on the basis of the positions of the Kirkendall planes and the point where $v \approx 0$ (sudden change in contrast) relative to the phase boundaries. Three intersections between the velocity curve and the line $v = x/2t$ (K_1, K_2 and K_3) are found, of which only two correspond to stable Kirkendall planes (at K_1 and K_3). (The position $x = 0$ represents the Matano plane.)

intermetallic containing 64 at.% Zn. ThO_2 particles (0.5–5μm) were used as fiducial markers between the initial end members. One sees that the inert particles rearranged upon interaction into two distinct marker planes (i.e. two Kirkendall planes) moving with different velocities within the newly formed layer of the β′-AuZn phase.

Another interesting feature that can be noticed from this back-scattered electron micrograph is the abrupt change in contrast near the equiatomic composition in the product layer. This is caused by the steep concentration gradient developed inside the β′-AuZn phase upon interdiffusion. The physical meaning of the existence of this gradient is the slow diffusion in the near-stoichiometric intermetallic AuZn, which reflects the highest degree of order in the B2 structure of the β′ phase in this composition interval (Gupta and Lieberman 1971, Hildegieck and Herzig 1983). This is also the position where $D_{Au} \approx D_{Zn}$ and, thus, where $v \approx 0$.

The corresponding velocity curve (that was constructed on the basis of positions of the Kirkendall planes $K_1$and K_3 and the point where $v \approx 0$ $(D_{Au} \approx D_{Zn})$ relative to the phase boundaries) is shown in figure 1 (*b*). Apparently, there is no theoretical restriction for the straight line $v = x/2t$ to intersect a Kirkendall velocity curve of such a shape up to three times as shown in this figure. This would, in principle, result in the appearance within the reaction product layer of three 'Kirkendall marker planes' that move parabolically in time. At first sight this would mean that the inert particles (markers) originally introduced at the contact surface of the couple would show up as three separate rows at the well-defined locations K_1, K_2 and K_3 inside the β′ intermetallic layer.

From a phenomenological standpoint, the appearance of a distinct Kirkendall marker plane at a specific position of a diffusion zone suggests that this plane of fixed (constant in time) composition can be viewed as some sort of an 'attractor' for markers. During interdiffusion, such 'attractor' accumulates the markers in its vicinity. It implies that for a Kirkendall plane to show up as a straight distinct row of markers, that is to be microstructurally stable (in space and time), the corresponding Kirkendall velocity near the location of the marker plane must have a negative gradient with respect to the position parameter. Indeed, in such a case, if markers (for whatever perturbations) appear slightly ahead of the Kirkendall plane position, they would slow down (lower velocity) and, if markers were slightly behind this position, they would move more rapidly (higher velocity).

Following a similar line of argument, it is clear that a Kirkendall marker plane is unstable during interdiffusion when the gradient at a point of intersection between the Kirkendall velocity curve and the line $v = x/2t$ is positive. Obviously, in the example considered here, only two of the three mathematically possible 'Kirkendall planes' can be found experimentally within the interaction zone. The unstable marker plane K_2 is situated between two stable Kirkendall planes K_1 and K_3, and the stable planes will trap all markers at the initial stage of the interdiffusion.

3.2. *General criterion of Kirkendall plane instability*

As explained in the preceding section, a Kirkendall plane is considered to be microstructurally unstable if at its location x_K in a diffusion zone, the corresponding marker velocity has a positive gradient, that is

$$\left.\frac{\partial v}{\partial x}\right|_{x_K} > 0. \tag{3}$$

Since we are dealing with a diffusion-controlled interaction, the instability criterion in a binary A–B system can be rewritten using equation (1) and the Boltzmann variable $\lambda = x/t^{1/2}$ as

$$\frac{\mathrm{d}}{\mathrm{d}\lambda}\left((D_\mathrm{B} - D_\mathrm{A})V_\mathrm{B}\,\frac{\mathrm{d}C_\mathrm{B}}{\mathrm{d}\lambda}\right)_{\lambda_K} > 0, \tag{4}$$

where λ_K corresponds to the Kirkendall plane location. Combining this inequality and Fick's second law in a form

$$-\frac{\lambda}{2}\,\frac{\mathrm{d}C_\mathrm{B}}{\mathrm{d}\lambda} = \frac{\mathrm{d}}{\mathrm{d}\lambda}\left(\tilde{D}\,\frac{\mathrm{d}C_\mathrm{B}}{\mathrm{d}\lambda}\right)$$

with $\tilde{D}$ being the interdiffusion coefficient defined as $\tilde{D} = C_\mathrm{A}V_\mathrm{A}D_\mathrm{B} + C_\mathrm{B}V_\mathrm{B}D_\mathrm{A}$ (Darken 1948), we arrive at the following expression:

$$\frac{\mathrm{d}}{\mathrm{d}\lambda}\left(\frac{D_\mathrm{B} - D_\mathrm{A}}{\tilde{D}}\,V_\mathrm{B}\right)\tilde{D}\,\frac{\mathrm{d}C_\mathrm{B}}{\mathrm{d}\lambda}\bigg|_{\lambda_\mathrm{K}} + \frac{D_\mathrm{B} - D_\mathrm{A}}{\tilde{D}}\,V_\mathrm{B}\,\frac{\mathrm{d}}{\mathrm{d}\lambda}\left(\tilde{D}\,\frac{\mathrm{d}C_\mathrm{B}}{\mathrm{d}\lambda}\right)_{\lambda_\mathrm{K}} > 0 \tag{5}$$

or further

$$\frac{\mathrm{d}}{\mathrm{d}C_\mathrm{B}}\left(\frac{D_\mathrm{B} - D_\mathrm{A}}{\tilde{D}}\,V_\mathrm{B}\right)\bigg|_{C_\mathrm{K}}\left(\frac{\mathrm{d}C_\mathrm{B}}{\mathrm{d}\lambda}\right)^2_{\lambda_\mathrm{K}} - \frac{\lambda_\mathrm{K}}{2}\,\frac{\mathrm{d}C_\mathrm{B}}{\mathrm{d}\lambda}\bigg|_{\lambda_\mathrm{K}}\,\frac{D_\mathrm{B} - D_\mathrm{A}}{\tilde{D}}\,V_\mathrm{B} > 0, \tag{6}$$

with C_K corresponding to the position of the Kirkendall plane.

Apparently, at the position of the Kirkendall plane ($x = x_\mathrm{K}$), the right-hand sides of equations (1) and (2) are equal. This can be restated as

$$\frac{\lambda_\mathrm{K}}{2} = (D_\mathrm{B} - D_\mathrm{A})V_\mathrm{B}\,\frac{\partial C_\mathrm{B}}{\partial\lambda}\bigg|_{\lambda_\mathrm{K}}. \tag{7}$$

Substituting equation (7) into equation (6), one obtains the following:

$$\tilde{D}\left(\frac{\mathrm{d}C_\mathrm{B}}{\mathrm{d}\lambda}\right)^2\left[\frac{\mathrm{d}}{\mathrm{d}C_\mathrm{B}}\left(\frac{D_\mathrm{B} - D_\mathrm{A}}{\tilde{D}}\,V_\mathrm{B}\right) - \left(\frac{D_\mathrm{B} - D_\mathrm{A}}{\tilde{D}}\,V_\mathrm{B}\right)^2\right] > 0. \tag{8}$$

After some algebra we have

$$\frac{\mathrm{d}}{\mathrm{d}C_\mathrm{B}}\left(\frac{\tilde{D}}{(D_\mathrm{B} - D_\mathrm{A})V_\mathrm{B}}\right) < -1. \tag{9}$$

Taking for simplicity $V_\mathrm{A} = V_\mathrm{B} = V_\mathrm{m}$, the instability criterion for the Kirkendall marker plane in a binary system is found as the simple expression

$$\frac{\mathrm{d}}{\mathrm{d}N_\mathrm{B}}\left(\frac{D_\mathrm{A}}{D_\mathrm{B}}\right)\bigg|_{N_\mathrm{K}} < 0, \tag{10}$$

where N_B is the mole fraction of component B. In words, this means that, when a Kirkendall plane is expected within a concentration range where the ratio of intrinsic diffusivities of A and B decreases with increasing concentration of B, it will be unstable. Condition (10) is a useful tool in finding candidates for Kirkendall plane instability.

3.3. *Appearance of a single, stable or an unstable Kirkendall marker plane in the growing* β'-*AuZn layer*

It is important to realize that the number of intersections between the Kirkendall velocity curve and the line $v = x/2t$ not only is determined by the shape of the curve but also depends on the position of the Matano plane ($x = 0$) in the diffusion couple. For instance, if one adds Zn to the pure Au end member of the diffusion couple discussed before, the position of the Matano plane shifts towards the Zn side of the reaction zone. Then, a situation may occur when the straight line $v = x/2t$ intersects the velocity curve, instead of three times, only once as is shown in figure 2 (*a*). One can see that the intersection point and, hence, the corresponding stable Kirkendall plane should be found at the Zn-rich part of the β′-AuZn product layer.

A typical example of such a situation is given in figure 2 (*b*), showing a diffusion zone of a reaction couple annealed at 500°C composed of γ-'AuZn$_2$' with a nominal composition $Au_{36}Zn_{64}$ and a two-phase alloy $Au_{66}Zn_{34}$. The latter alloy after equilibration at 500°C consists of a saturated (Au, Zn) solid solution and precipitates of the β′ phase. The sudden change in contrast at the near-stoichiometric composition in the newly formed β′-AuZn intermetallic is again clearly visible in the micrograph. As expected, the ThO_2 particles used as inert markers between the couple halves are found as a straight row of inclusions at one specific position (point K in figure 2 (*a*)) in the Zn-rich of the β′-phase layer.

The marker plane is also revealed by the differences in grain morphology inside the β′ layer. The differently nucleated grains of the product phase meet at the Kirkendall plane. Therefore, this plane can readily be seen within the reaction layer even without the presence of any inert particles.

Extending this approach further, it can be understood that, if the position of the Matano plane shifts in the direction of the Au side of the incremental couple, the stable Kirkendall marker plane will appear in the Au-rich domain of the β′-AuZn intermetallic layer. This is demonstrated in figure 3 (*a*). Here, experimental proof came from the analysis of the diffusion zone morphology developed during interaction (500°C; 16 h; Ar + 5 vol.% H_2) between pure Au and an equilibrated $Au_{40}Zn_{60}$ alloy consisting of a γ-'AuZn$_2$' matrix phase and β′ precipitates (figure 3 (*b*)). As predicted, the Kirkendall marker plane appears in the Au-rich part of the β′-AuZn product layer.

Obviously, one more possible configuration of the marker velocity construction can be envisaged, in which the line $v = x/2t$ intersects the velocity curve only once, but at a point where the gradient of the Kirkendall velocity is positive, for example as shown in figure 4 (*a*). In this case, the predicted Kirkendall marker plane is microstructurally unstable, and no stable Kirkendall plane is present next to the unstable plane, that is no 'attractor' for markers exists in the diffusion zone. Therefore, no well-defined Kirkendall marker plane will develop upon interdiffusion in such a system.

A very telling example of the Kirkendall plane instability is provided by the experiments on a diffusion couple consisting of an equilibrated two-phase γ-AuZn$_2$ + β′-AuZn alloy with nominal composition $Au_{40}Zn_{60}$ and a $Au_{70}Zn_{30}$ solid solution. A representative microstructure of the couple after annealing at 500°C for 6 h under flowing Ar + 5 vol.% H_2 gas mixture is given in figure 4 (*b*). Unlike the previous cases, no distinct row of the ThO_2 inclusions used as fiducial markers between the end members can be seen inside the product phase β′-AuZn. However, close inspection of the intermetallic layer in the vicinity of the expected

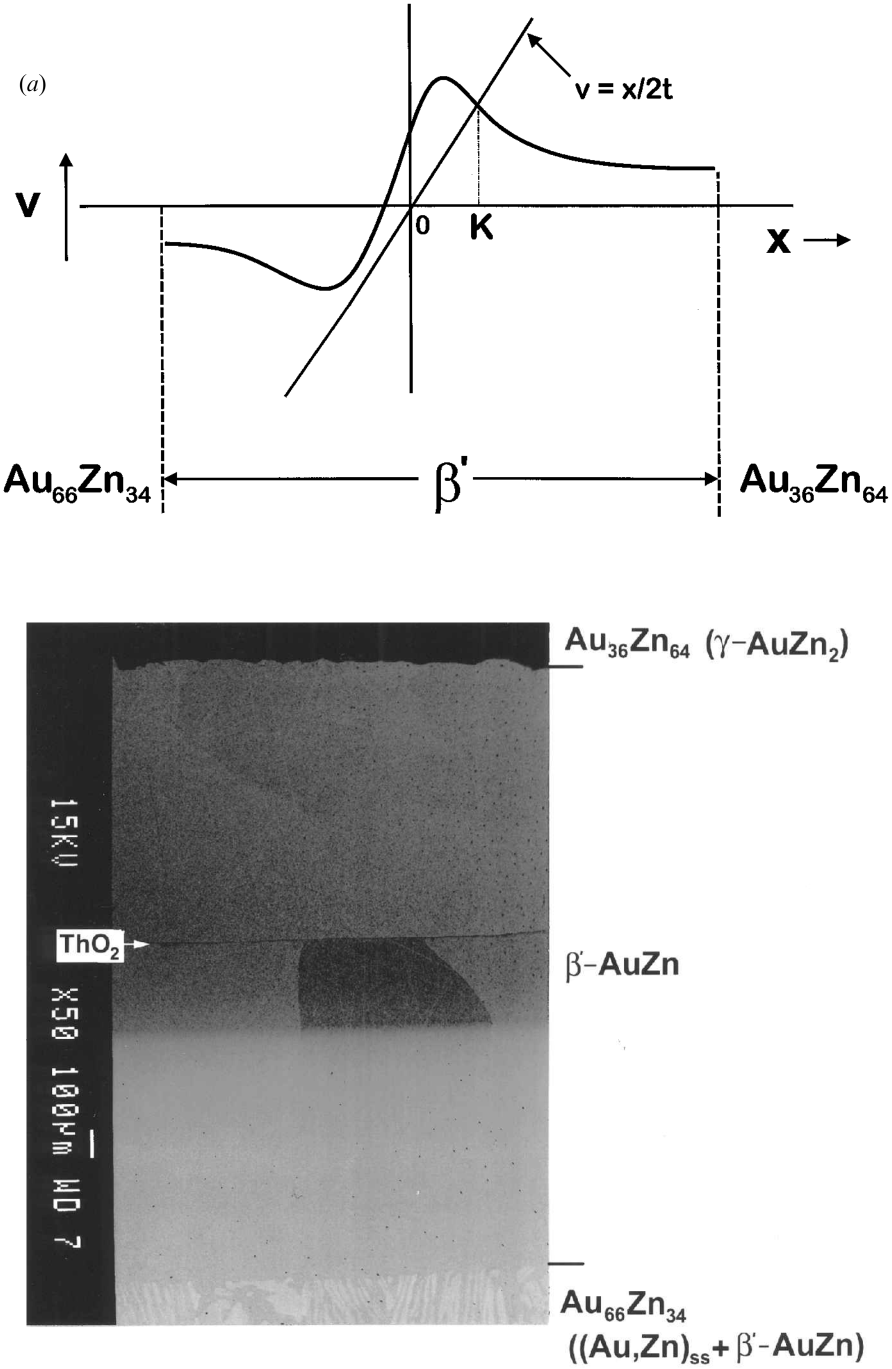

(*b*)

Figure 2. (*a*) The Kirkendall velocity curve corresponding to the product layer of the β′-AuZn intermetallic formed during reaction between γ-‘$AuZn_2$’ ($Au_{36}Zn_{64}$) and a two-phase $Au_{66}Zn_{34}$ alloy ((Au, Zn) solid solution +β′-AuZn) (500°C; 17 h; Ar + 5 vol.% H_2). The straight line $v = x/2t$ intersects the velocity curve only once at the Zn-rich side of the β′-AuZn layer. (*b*) BEI of the diffusion zone after annealing.

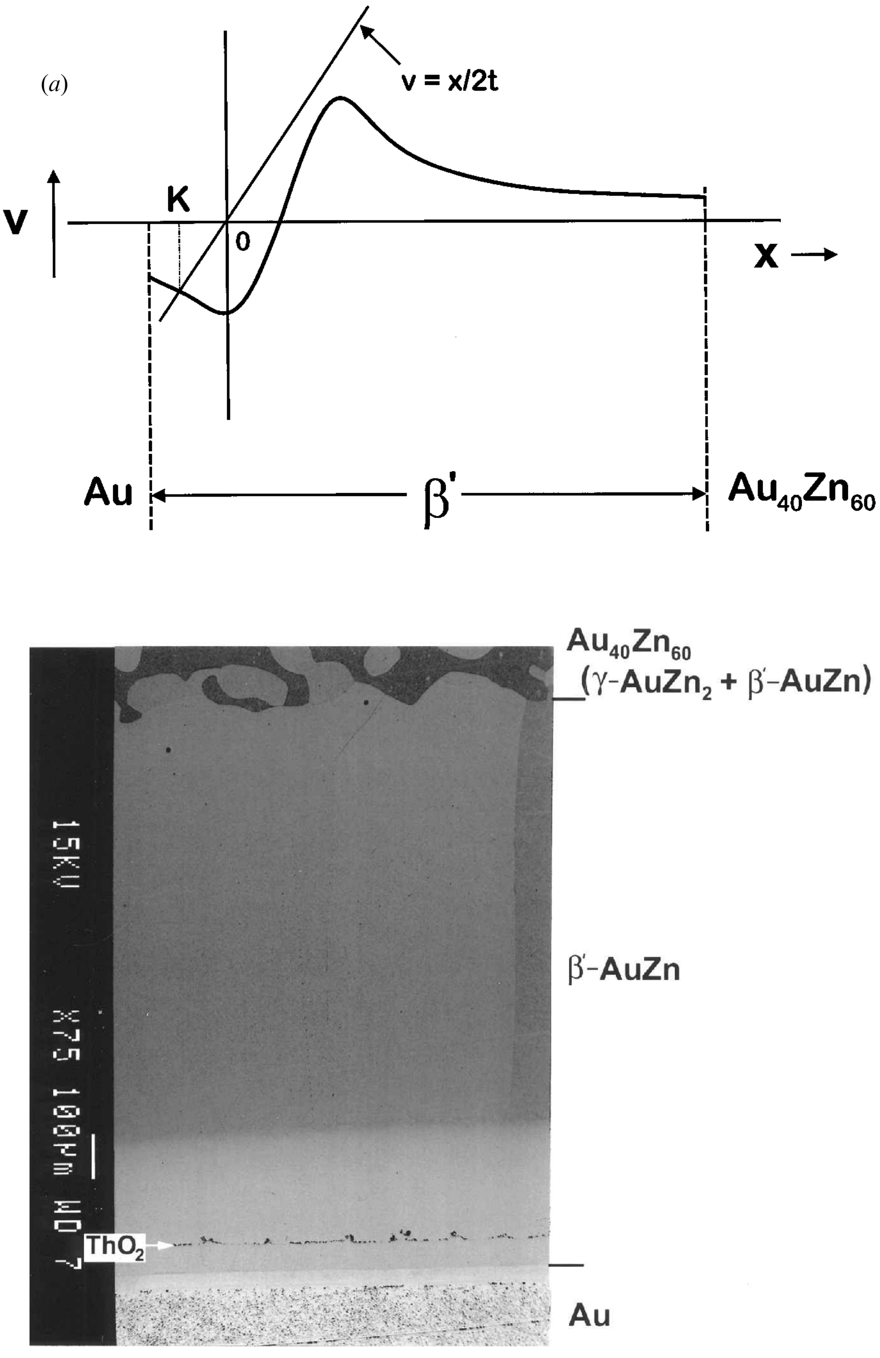

(*b*)

Figure 3. (*a*) The Kirkendall velocity construction corresponding to the layer of β′-AuZn diffusion grown at 500°C for 17.5 h in Ar + 5 vol.% H_2 between Au and a $Au_{40}Zn_{60}$ two-phase alloy (γ-'$AuZn_2$' + β′-AuZn). Only one Kirkendall marker plane appears in the Au-rich part of the product layer. (*b*) Corresponding microstructure of the reaction zone (BEI).

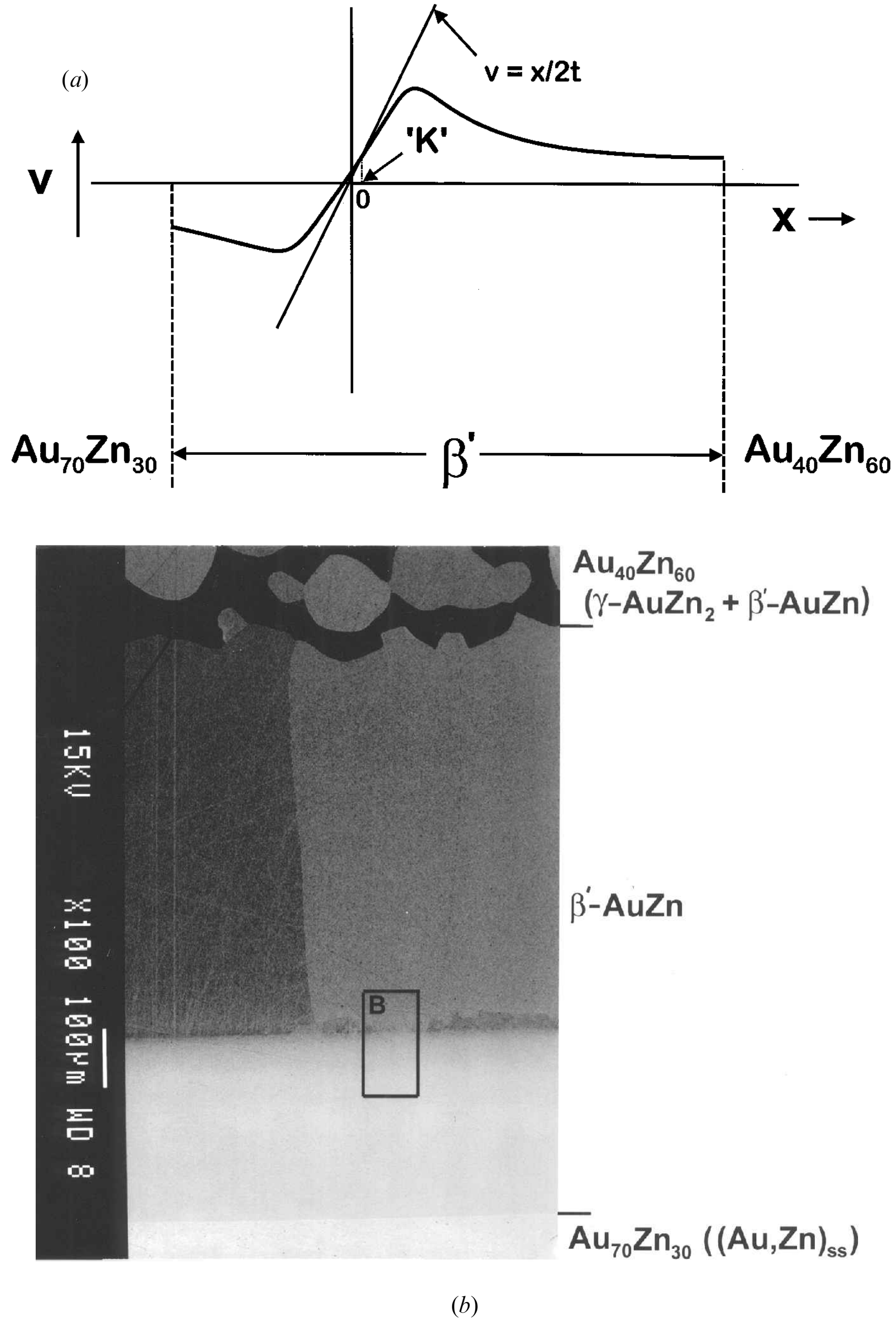

Figure 4. (*a*) The Kirkendall velocity curve corresponding to the diffusion-grown layer of β′-AuZn in a $Au_{70}Zn_{30}$–$Au_{40}Zn_{60}$ reaction couple (500°C; 6 h; Ar + 5 vol.% H_2). The line $v = x/2t$ intersects the velocity curve at a position 'K' where the gradient of the Kirkendall velocity is positive. The corresponding 'Kirkendall' plane is unstable. The scattered array of the ThO_2 markers formed upon interdiffusion results from the Kirkendall plane instability. (*b*) Corresponding microstructure of the reaction zone (BEI). (*c*) Magnified area (B in (*b*)) of the product layer in the vicinity of the unstable Kirkendall plane location (BEI).

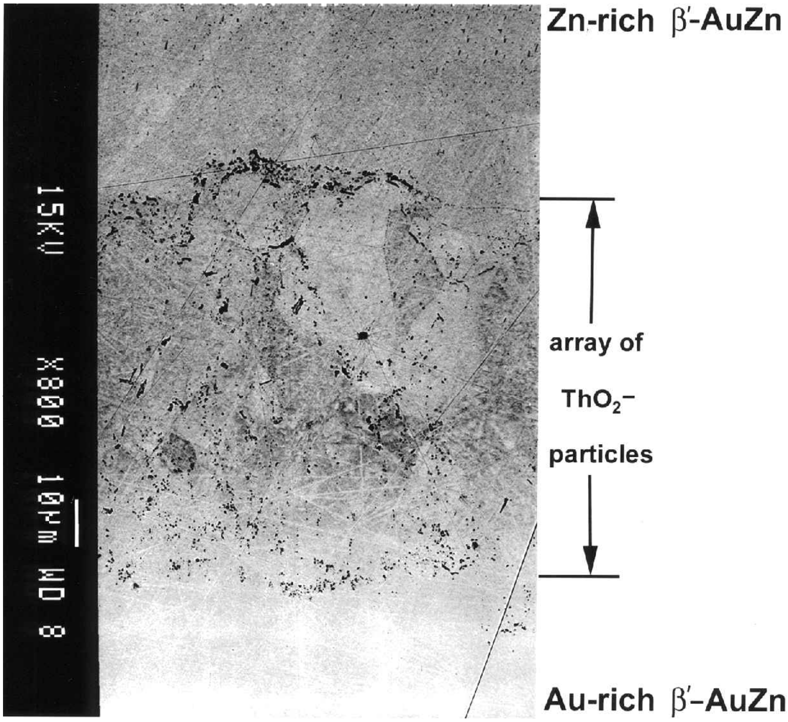

(*c*)

Figure 4. (*continued*)

location of the unstable Kirkendall plane revealed the occurrence of the ThO_2 inclusions spatially distributed in the diffusion direction (figure 4 (*c*)). It looks like the system 'forgot' the initial contact interface.

§ 4. CONCLUDING REMARKS

No further proof is necessary to demonstrate that, in a diffusion-controlled interaction, the Kirkendall plane as marked by inert particles placed at the original contact surface of a reaction couple, need not be unique. Multiple planes can emerge during interdiffusion in a single-phase reaction product layer and, in some cases, the Kirkendall marker plane does not exist at all.

A purely phenomenological approach was presented to explain the Kirkendall-effect induced migration of inert markers inside the reaction layer of β′-AuZn phase. It was shown that number, location and micro-structural stability of the marker planes within the product intermetallic can be rationalized (on a qualitative level) using the concept of the Kirkendall velocity construction.

At this stage, no attempts were made to propose any atomic mechanism responsible for the observed behaviour of inert inclusions during interdiffusion.

An important question that remains to be answered is concerned with the spatial distribution of the inert particles in the vicinity of the unstable Kirkendall plane location when no 'attractors' for markers exist in a diffusion zone. Research currently under way will, if successful, enable us to compute and experimentally to verify the evolution (spatial and temporal) of the marker distribution around the unstable ('virtual') Kirkendall plane. In this respect, experiments on materials with a well-defined initial distribution of fiducial markers across the anticipated interdiffusion zone may elucidate this peculiar solid-state phenomenon.

ACKNOWLEDGEMENT

The expert technical assistance provided by Huub van der Palen is greatly appreciated.

REFERENCES

CORNET, J.-F., and CALAIS, D., 1972, *J. Phys. Chem. Solids,* **33**, 1675.

DARKEN, L. S., 1948, *Trans. AIME,* **175**, 184.

DARUKA, I., SZABÓ, I. A., BEKE, D. L., CSERHÁTI, C., KODENTSOV, A. A., and VAN LOO, F. J. J., 1996, *Acta mater.,* **44**, 4981.

GUPTA, D., and LIEBERMAN, D. S., 1971, *Phys. Rev.* B, **4**, 1070.

HILGEDIECK, R., and HERZIG, C., 1983, *Z. Metallk.,* **74**, 38.

KODENTSOV, A. A., RIJNDERS, M. R., and VAN LOO, F. J. J., 1998, *Acta mater.,* **46**, 6521.

OKAMOTO, H., and MASSALSKI, T. B., 1988, *Phase Diagrams of Binary Gold Alloys* (Metals Park, Ohio: American Society for Metals), p. 331.

PHILIBERT, J., 1991, *Atom Movements-Diffusion and Mass Transport in Solids* (Les Ulis: Les Éditions de Physique), p. 211.

SHIMOZAKI, T., GODA, Y., WAKAMATSU, Y., and ONISHI, M., 1993, *Defect Diffusion Forum,* **95–98**, 629.

SMIGELSKAS, A. D., and KIRKENDALL, E. O., 1947, *Trans. AIME,* **171**, 130.

STEPHENSON, G. B., 1988, *Acta metall.,* **36**, 2663.

VAN DAL, M. J. H., KODENTSOV, A. A., and VAN LOO, F.J.J., 2000a, *Solid St. Phenomena,* **72**, 111.

VAN DAL, M. J. H., PLEUMEEKERS, M. C. L. P., KODENTSOV, A. A., and VAN LOO, F. J. J., 2000b, *Acta mater.,* **48**, 385.

VAN LOO, F. J. J., PIERAGGI, B., and RAPP, R. A., 1990, *Acta metall. mater.,* **38**, 1769.